Contents

Chapter 1

Theory

1.1 The induced electric field equation

The electromagnetic field generated by the current density flowing through the coil, J_{coil}, and that induced in the plasma, J_{ind}, is governed by the Maxwell's equations

$$\nabla \cdot \boldsymbol{E} = \frac{\rho}{\epsilon_0} \tag{1.1a}$$

$$\nabla \cdot \boldsymbol{B} = 0 \tag{1.1b}$$

$$\nabla \times \boldsymbol{E} = -\frac{\partial \boldsymbol{B}}{\partial t} \tag{1.1c}$$

$$\nabla \times \boldsymbol{B} = \mu_0 \left(\boldsymbol{J_{coil}} + \boldsymbol{J_{ind}} \right) + \epsilon \mu_0 \frac{\partial \boldsymbol{E}}{\partial t} \tag{1.1d}$$

where $\boldsymbol{E}$ and $\boldsymbol{B}$ are the three-dimensional components of the electric and magnetic fields, μ_0 and ϵ_0 the permeability and permittivity of the free space and ρ the charge density. The charge density ρ is supposed null because the excitation frequency is by far smaller than the fundamental frequency of the plasma, which leads to a quasi-neutral state of the plasma. Furthermore the displacement current can also be neglected, which is done by splitting the electric field E into the induced electric field E_{ind} and the electric field generated by the coils E_{coils}. The term $\epsilon\mu_0 \partial E_{ind}/\partial t$ is removed by neglecting the electromagnetic waves and the term $\epsilon\mu_0 \partial E_{coil}/\partial t$ is removed by neglecting the electric oscillations. The Maxwell's equations boil down to

$$\nabla \cdot \boldsymbol{E} = 0 \tag{1.2a}$$

$$\nabla \cdot \boldsymbol{B} = 0 \tag{1.2b}$$

$$\nabla \times \boldsymbol{E} = -\frac{\partial \boldsymbol{B}}{\partial t} \tag{1.2c}$$

$$\nabla \times \boldsymbol{B} = \mu_0 \left(\boldsymbol{J_{coil}} + \boldsymbol{J_{ind}} \right) \tag{1.2d}$$

It is convenient to introduce the magnetic vector potential $\boldsymbol{A}$

$$\boldsymbol{B} = \nabla \times \boldsymbol{A} \tag{1.3}$$

which, introduced in the Maxwell's equations, lead to

$$\boldsymbol{E} = -\frac{\partial \boldsymbol{A}}{\partial t} \tag{1.4a}$$

$$\nabla^2 \boldsymbol{A} = -\mu_0 \left(\boldsymbol{J_{coil}} + \boldsymbol{J_{ind}} \right) \tag{1.4b}$$

The induced current density is expressed by the simplified Ohm's law

$$\boldsymbol{J_{ind}} = \sigma \boldsymbol{E} = -\sigma \frac{\partial \boldsymbol{A}}{\partial t} \tag{1.5}$$

Further simplifications are made by assuming a sinusoidal time variation with frequency f. The classical complex notation is then used to eliminate the time variable from Eq. (1.4b). To do so let us define

$$\boldsymbol{J_{coil}}(\boldsymbol{r}, t) = \Re\left\{\widetilde{\boldsymbol{J}}_{\boldsymbol{coil}}(\boldsymbol{r}) e^{i\omega t}\right\} \tag{1.6a}$$

$$\boldsymbol{A}(\boldsymbol{r}, t) = \Re\left\{\widetilde{\boldsymbol{A}}(\boldsymbol{r}) e^{i\omega t}\right\} \tag{1.6b}$$

with $\widetilde{\boldsymbol{J}}_{\boldsymbol{coil}}$ and $\widetilde{\boldsymbol{A}}$ the phasors and $\omega = 2\pi f$. One then gets

$$\nabla^2 \widetilde{\boldsymbol{A}} - i\mu_0\sigma\omega \widetilde{\boldsymbol{A}} = -\mu_0 \widetilde{\boldsymbol{J}}_{\boldsymbol{coil}} \tag{1.7}$$

Under the assumption of an axisymmetric configuration for the induction circuit, the electric current density flowing in the coil and, consequently, the magnetic vector potential will only have tangential components. The electric current density $\widetilde{\boldsymbol{J}}_{\boldsymbol{coil}}$ is purely real so that

$$\widetilde{\boldsymbol{J}}_{\boldsymbol{coil}} = J_{coil} \overline{\boldsymbol{e}}_\theta \tag{1.8a}$$

$$\widetilde{\boldsymbol{A}} = \left(A_\theta^r + iA_\theta^i\right) \overline{\boldsymbol{e}}_\theta \tag{1.8b}$$

$$\widetilde{\boldsymbol{E}} = \left(E_\theta^r + iE_\theta^i\right) \overline{\boldsymbol{e}}_\theta = \omega\left(A_\theta^i - iA_\theta^r\right) \overline{\boldsymbol{e}}_\theta \tag{1.8c}$$

Equation (1.7) can then be expressed in terms of electric field and be split into the followings

$$\frac{1}{r}\frac{\partial}{\partial r}\left(r\frac{\partial E_\theta^r}{\partial r}\right) + \frac{\partial^2 E_\theta^r}{\partial z^2} - \frac{E_\theta^r}{r^2} + \mu_0\sigma\omega E_\theta^i = 0 \tag{1.9a}$$

$$\frac{1}{r}\frac{\partial}{\partial r}\left(r\frac{\partial E_\theta^i}{\partial r}\right) + \frac{\partial^2 E_\theta^i}{\partial z^2} - \frac{E_\theta^i}{r^2} - \mu_0\sigma\omega E_\theta^r = \mu_0\omega J_{coil} \tag{1.9b}$$

Provided that J_{coil} is known, equations (1.9a)- (1.9b) can be solved to calculate the induced electric field. The magnetic field can then be retrieved through Eq. (1.2c)

$$B_z = B_{zr} + iB_{zi} = \frac{1}{i\omega}\frac{\partial(E_\theta^r + iE_\theta^i)}{\partial z} = \frac{1}{\omega}\frac{\partial(E_\theta^i - iE_\theta^r)}{\partial z} \tag{1.10a}$$

$$B_r = B_{rr} + iB_{ri} = -\frac{1}{i\omega}\frac{1}{r}\frac{\partial r(E_\theta^r + iE_\theta^i)}{\partial r} = \frac{1}{\omega}\frac{1}{r}\frac{\partial r(-E_\theta^i + iE_\theta^r)}{\partial r} \tag{1.10b}$$

If an electric current $I_{coil} = J_{coil}\Omega_{coil}$ flows through the coils of section Ω_{coil}, then one can explicit the right-hand side of Eq. (1.9b). The outer inductor is approximated by a series of n_r parallel rings of radius R_i and axial position Z_i

$$J_{coil}(z,r) = \sigma E_{coil}(z,r) = -i\omega\sigma A_{coil}(z,r) = -i\omega\sigma\frac{\mu_0 I_c}{2\pi}\sum_{i=1}^{n_r}\sqrt{\frac{R_i}{r}}G(m) \tag{1.11a}$$

$$G(m) = \frac{(2-m)K(m) - 2E(m)}{\sqrt{m}} \tag{1.11b}$$

$$m = \frac{4rR_i}{(r+R_i)^2 + (Z_i - z)^2} \tag{1.11c}$$

with $K(m)$ and $E(m)$ being the elliptic integrals of first and second kind, respectively. The reader can find the building of the previous relations in Section 1.3.

1.2 Boundary conditions

The induced electric field must satisfy boundary conditions so that the system of equations built by the numerical method can be solved. On the axis, because of the axisymmetric hypothesis, the vanishing condition is imposed

$$E_\theta(z, 0) = 0 \tag{1.12}$$

Two approaches exist in terms of type of computational domain and associated boundary conditions. A first common configuration computes the electric field inside the torch only. This approach, introduced by McKelliget [1], solves the induction equations (1.9) inside the torch, each element inside the torch being considered as an infinitely thin current-carrying loop. The electric field on the boundary of the torch is obtained by summing up all the contributions coming from both excitation and induced currents flowing in the coil and in the plasma, respectively. Although mathematically elegant, this integral boundary procedure is computationally expensive, as it couples every boundary cell to all interior cells. Moreover, due to the term accounting for the effects of the induced currents, the whole distribution of E_θ in the plasma region needs to be known to determine the vector potential at each point on the boundaries. Thus, an iterative approach has to be employed to solve the electromagnetic field equations, leading to slow convergence of the numerical process. This approach will not be implemented in this project.

Another approach uses a computational grid which extends well outside the plasma discharge region, so that simpler boundary conditions can be adopted for the electric field. Vanden Abeele [2] and Lopes [3] rely on a sufficiently large enough external domain to impose the vanishing conditions

$$E_\theta(z, r) = 0 \qquad \text{if the external domain is large enough} \tag{1.13}$$

Bernardi *et al.* [4] introduced a new concept that allows the external domain to be considerably smaller without affecting the quality of the solution. The border of the external domain have been placed far enough from the plasma region in order to use boundary conditions for the electric field as if the torch were a magnetic dipole produced by the electric current flowing in the plasma and in the induction coil. Far enough away from the discharge, the whole system can be treated as a single magnetic dipole placed at the mid-coil point, with momentum parallel to the axis of the torch. Under such an assumption and taking a cylindrical (z, r) reference frame with the origin at the dipole and z-axis parallel to its momentum, the electric field at sufficient distance from the torch is given by the classic expression:

$$E_\theta(z, r) = C \frac{r}{(r^2 + z^2)^{(3/2)}} \tag{1.14}$$

In the later relation, C is a constant which accounts for the momentum of the dipole, whose value is not known *a priori* as it depends upon the induced currents which, in turn, depend upon the electric field in the discharge region. However, the value of C is not actually required for our purposes. By taking the $z-$ and $r-$derivatives of Eq. (1.14) and eliminating the unknown constant C, one obtains boundary conditions to be applied on the external domain:

$$\frac{\partial E_\theta}{\partial z} = -\frac{3z}{r^2 + z^2} E_\theta \tag{1.15a}$$

$$\frac{\partial E_\theta}{\partial r} = \frac{1 - 3r^2 (r^2 + z^2)^{-1}}{r} E_\theta \tag{1.15b}$$

1.3 Electric field generated by a single coil

Chapter 2

Numerical discretization

2.1 Finite element method

2.1.1 General considerations

The finite element (FE) method introduces the concept representation of the solution by functions. The spatial domain is discretized into elements of chosen shapes (triangles, quadrangles, etc.) and equations (1.9a) and (1.9b) are solved at the corners of these elements. The solution can be interpolated inside the elements through shape functions $N_j(r,z)$, for which the order will fix the precision of the result. The solution at any point in the two-dimensional space is then based on the knowledge of the solution E_j at the corners of the elements:

$$E(z,r) = \sum_k N_k(z,r) E_k \tag{2.1}$$

The numerical discretization of the physical equations does not allow the strict respect of the left-hand side being equal to the right-hand side. A residual is introduced in the physical equations. The FE method is based on the weighted minimalisation of the residual over the whole domain. In order to defined the discretized equation at node j, the Galerkin FE method picks the shape function at that node $N_j(z,r)$ as the weight factor:

$$2\pi \int_\Omega r N_j(z,r) \left(\nabla^2 \widetilde{\boldsymbol{E}}_j - i\mu_0\sigma\omega\widetilde{\boldsymbol{E}}_j - i\mu_0\omega\widetilde{\boldsymbol{J}}_{\boldsymbol{coil}j} \right) drdz = 0 \tag{2.2}$$

The shape functions are null everywhere except at the node j of interest. The choice of the Galerkin method has the consequence that only the direct neighbour nodes k are involved in the discretized equations at node j. These shape functions are moreover of order one because no special physical behaviour is expected.

2.1.2 Galerkin finite element equations

Assuming an implicit summation over the index k, one can write down the Galerkin FE discretization of equations (1.9a) and (1.9b) at node j as

$$\int_\Omega rN_j \left(\frac{1}{r}\frac{\partial}{\partial r}\left(r\frac{\partial N_k}{\partial r}\right) E^r_{\theta k} + \frac{\partial^2 N_k}{\partial z^2} E^r_{\theta k} - \frac{N_k E^r_{\theta k}}{r^2} + \mu_0\sigma\omega N_k E^i_{\theta k} \right) drdz = 0 \tag{2.3a}$$

$$\int_\Omega rN_j \left(\frac{1}{r}\frac{\partial}{\partial r}\left(r\frac{\partial N_k}{\partial r}\right) E^i_{\theta k} + \frac{\partial^2 N_k}{\partial z^2} E^i_{\theta k} - \frac{N_k E^i_{\theta k}}{r^2} - \mu_0\sigma\omega N_k E^r_{\theta k} - \mu_0\omega J_{coil} \right) drdz = 0 \tag{2.3b}$$

Integrating by part the two first terms of each equation allows the usage of shape functions of first order:

$$\int_\Omega \left(-r\frac{\partial N_j}{\partial r}\frac{\partial N_k}{\partial r}E^r_{\theta k} - r\frac{\partial N_j}{\partial z}\frac{\partial N_k}{\partial z}E^r_{\theta k} - \frac{N_j N_k E^r_{\theta k}}{r} + \mu_0\sigma\omega r N_j N_k E^i_{\theta k} \right) drdz \\ + \underbrace{\int_{\partial\Omega} \left(rN_j n_r \frac{\partial E^r_\theta}{\partial r} + rN_j n_z \frac{\partial E^r_\theta}{\partial z} \right) d\Gamma}_{=\int_{\partial\Omega} rN_j \frac{\partial E^r_\theta}{\partial n} d\Gamma \text{ far field condition}} = 0 \tag{2.4a}$$

$$\int_\Omega \left(-r\frac{\partial N_j}{\partial r}\frac{\partial N_k}{\partial r}E^i_{\theta k} - r\frac{\partial N_j}{\partial z}\frac{\partial N_k}{\partial z}E^i_{\theta k} - \frac{N_j N_k E^i_{\theta k}}{r} - \mu_0\sigma\omega r N_j N_k E^r_{\theta k} - \mu_0\omega r N_j J_{coil} \right) drdz \\ + \underbrace{\int_{\partial\Omega} \left(rN_j n_r \frac{\partial E^i_\theta}{\partial r} + rN_j n_z \frac{\partial E^i_\theta}{\partial z} \right) d\Gamma}_{=\int_{\partial\Omega} rN_j \frac{\partial E^i_\theta}{\partial n} d\Gamma \text{ far field condition}} = 0 \tag{2.4b}$$

Note that the boundary integrals make appear the $z-$ and $r-$ derivatives of the electric field, which were specified in Eqs. (1.15). Taking into account that information, the boundary integral for the real component (and similarly for the imaginary one) becomes

$$\int_{\partial\Omega} rN_j \frac{\partial E^r_\theta}{\partial n} d\Gamma = \int_{\partial\Omega} N_j N_k \left(n_r \frac{(z-z_c)^2 - 2r^2}{r^2 + (z-z_c)^2} - 3n_z \frac{r(z-z_c)}{r^2+(z-z_c)^2} \right) E^r_{\theta k} d\Gamma \tag{2.5}$$

where z_c is the axial location of the mid-coil point. For the sake of clarity, let us define the following elemental matrices

$$m_{jk} = \int_\Omega rN_j N_k drdz \tag{2.6a}$$

$$k_{jk} = -\int_\Omega r \left(\frac{\partial N_j}{\partial r}\frac{\partial N_k}{\partial r} + \frac{\partial N_j}{\partial z}\frac{\partial N_k}{\partial z} \right) drdz \tag{2.6b}$$

$$p_{jk} = -\int_\Omega \frac{N_j N_k}{r} drdz \tag{2.6c}$$

$$s_{jk} = \int_{\partial\Omega} N_j N_k \left(n_r \frac{(z-z_c)^2 - 2r^2}{r^2+(z-z_c)^2} - 3n_z \frac{r(z-z_c)}{r^2+(z-z_c)^2} \right) d\Gamma \tag{2.6d}$$

These matrices are dependent on the shape functions only and can be evaluated through analytical expressions for some of them, or through numerical quadratures for others. Let us also use the same paradigm for the forcing term J_{coil} as for the unknown induced electric field: $J_{coil}(z,r) = \sum_k N_k(z,r) J_{coil,k}$. This allows the Galerkin FE to boil down to

$$(k_{jk} + p_{jk} + s_{jk})\, E^r_{\theta k} + \mu_0\sigma\omega m_{jk} E^i_{\theta k} = 0 \tag{2.7a}$$

$$(k_{jk} + p_{jk} + s_{jk})\, E^i_{\theta k} - \mu_0\sigma\omega m_{jk} E^r_{\theta k} = \mu_0\omega m_{jk} J_{coil,k} \tag{2.7b}$$

or in terms of matrix representation

$$\begin{pmatrix} k_{jk} + p_{jk} + s_{jk} & \mu_0\sigma\omega m_{jk} \\ -\mu_0\sigma\omega m_{jk} & k_{jk} + p_{jk} + s_{jk} \end{pmatrix} \begin{pmatrix} E^r_{\theta k} \\ E^i_{\theta k} \end{pmatrix} = \begin{pmatrix} 0 \\ \mu_0\omega m_{jk} J_{coil,k} \end{pmatrix} \tag{2.8}$$

The real and imaginary components are coupled through the term m_{jk}. In the case where the electrical conductivity σ of the medium is null, then only the imaginary component of the induced electric field is non-zero.

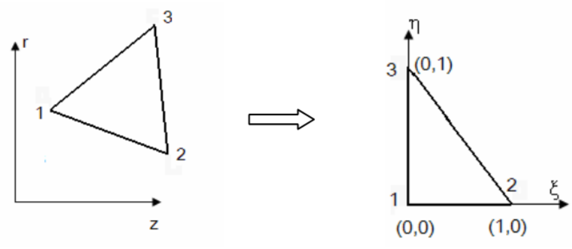

Figure 2.1.1: Definition of the triangular FE and its transformation to the (ξ, η) plane.

2.1.3 Elemental matrices for triangular elements

The analytical evaluation of the elemental matrices m_{jk} and k_{jk} is more easily performed in a new (η, ξ) plane defined in Fig. 2.1.1. Doing so the linear shape functions take the form

$$N_1(\eta, \xi) = 1 - \eta - \xi \tag{2.9a}$$
$$N_2(\eta, \xi) = \eta \tag{2.9b}$$
$$N_3(\eta, \xi) = \xi \tag{2.9c}$$

The integrals on this right triangle in (ξ, η) plane are related to the integrals on the true element (of area Ω) in the (z, r) plane by the Jacobian of the transformation which apply the element on the right triangle

$$\int_\Omega \psi(z,r)drdz = \int_0^1 \int_0^{1-\xi} \psi(\eta, \xi)|J(\xi, \eta)|d\eta d\xi \tag{2.10}$$

where $|J(\xi, \eta)|$ is the determinant of the Jacobian defined as

$$J(\eta, \xi) = \begin{pmatrix} \frac{\partial r}{\partial \xi} & \frac{\partial r}{\partial \eta} \\ \frac{\partial z}{\partial \xi} & \frac{\partial z}{\partial \eta} \end{pmatrix} \tag{2.11}$$

By choosing $\psi = 1$ one gets the relation $|J(\xi, \eta)| = 2\Omega$ which is easily computed. Let us define the normals of the segment on the other side of a node:

$$\boldsymbol{n}_1 = (r_3 - r_2)\overline{\boldsymbol{e}}_z + (z_2 - z_3)\overline{\boldsymbol{e}}_r \tag{2.12a}$$
$$\boldsymbol{n}_2 = (r_1 - r_3)\overline{\boldsymbol{e}}_z + (z_3 - z_1)\overline{\boldsymbol{e}}_r \tag{2.12b}$$
$$\boldsymbol{n}_3 = (r_2 - r_1)\overline{\boldsymbol{e}}_z + (z_1 - z_2)\overline{\boldsymbol{e}}_r \tag{2.12c}$$

Then the analytical expressions for the elemental matrices m_{jk} and k_{jk} are (see Detandt [5])

$$m_{jk} = \frac{\Omega(r_1 + r_2 + r_3 + r_j + r_k)(1 + \delta_{jk})}{60} \tag{2.13a}$$
$$k_{jk} = -\frac{(r_1 + r_2 + r_3)(n_j^r n_k^r + n_j^z n_k^z)}{12\Omega} \tag{2.13b}$$

The elemental matrix p_{jk} requires a numerical quadrature because of the difficulty to evaluate analytically. For this purpose, four internal quadrature points are taken in order to avoid any singularity at $r = 0$ (see Table 2.1):

$$p_{jk} = -\int_\Omega \frac{N_j N_k}{r} drdz = -\sum_{n=1}^{4} w_n \frac{N_j(\eta_n, \xi_n) N_k(\eta_n, \xi_n)}{r_n} |J(\xi, \eta)| \tag{2.14}$$

n	ξ	η	w	N_1	N_2	N_3	r
1	1/3	1/3	-27/96	1/3	1/3	1/3	$(r_1 + r_2 + r_3)/3$
2	0.2	0.6	25/96	0.2	0.2	0.6	$0.2(r_1 + r_2) + 0.6r_3$
3	0.6	0.2	25/96	0.2	0.6	0.2	$0.2(r_1 + r_3) + 0.6r_2$
4	0.2	0.2	25/96	0.6	0.2	0.2	$0.2(r_2 + r_3) + 0.6r_1$

Table 2.1: Quadrature table for the element matrix p_{jk}.

d	ξ	w
1 and 2	$\pm$0.8611363116	0.3478548451
3 and 4	$\pm$0.3399810436	0.6521451548

Table 2.2: Quadrature table for the element matrix s_{jk}.

2.1.4 Elemental matrices for edge elements

The boundary integral s_{jk} in Eq. (2.6) appears only on the nodes lying on the boundary of the external domain. The shape functions N_j and N_k are linear and (n_z, n_r) is the normal to the edge element, pointing outwards the domain. This elemental matrix is not simple and a numerical quadrature must be performed to compute it. To perform this numerical quadrature, the two nodes at (z_1, r_1) and (z_2, r_2) that define the edge element must be transformed to a new coordinate $-1 \leq \xi \leq 1$ through the relation

$$z = z_1 + \frac{\xi + 1}{2}(z2 - z1) \tag{2.15a}$$

$$r = r_1 + \frac{\xi + 1}{2}(r2 - r1) \tag{2.15b}$$

The shape functions are then given by

$$N_1(\xi) = \frac{1 - \xi}{2} \tag{2.16a}$$

$$N_2(\xi) = \frac{1 + \xi}{2} \tag{2.16b}$$

and the quadrature is approximated by

$$s_{jk} = \sum_{d=1}^{4} w_d N_j(\xi_d) N_k(\xi_d) \left(n_r \frac{(z_d - z_c)^2 - 2r_d^2}{r_d^2 + (z_d - z_c)^2} - 3n_z \frac{r(z_d - z_c)}{r_d^2 + (z_d - z_c)^2} \right) \frac{L}{2} \tag{2.17}$$

with $L = \sqrt{(z_2 - z_1)^2 + (r_2 - r_1)^2}$ being the length of the edge element and the quadrature points ξ_d and weights w_d are defined in Table 2.2.

Chapter 3

Numerical results

This chapter displays the results of the resolution of Equations (2.8) inside and around an inductively coupled plasma torch. The geometry of the whole domain and detail of the VKI minitorch are shown in Fig. 3.0.1. This minitorch has a diameter of $3cm$, an excitation frequency of 27MHz and works with argon. The following sections will study

- the influence of the radius R of the external domain,
- the influence of the type of boundary condition set at the far field,
- the convergence rate of the numerical method as a function of degrees of freedom inside the torch,
- the influence of the electrical conductivity σ on the solution,
- the influence of the excitation frequency f of the coils

3.1 Influence of the size of the external domain

The external domain surrounding the torch is a circle centered on the torch, of radius R (see Fig. 3.0.1). The radius R of the circle is increased from $0.1m$ to $1.0m$ by increment of $0.1m$ and the two types of boundary conditions on the outer boundary (Section 1.2) are tested here. Three values of the electrical conductivity are taken ($\sigma = 10^2$, 10^3 and $10^4 S/m$) and the excitation frequency is set to 27MHz.

The largest radius is chosen as reference and the relative error for both real and imaginary parts of the electric field is defined as

$$\epsilon_{rel} = \sqrt{\frac{\sum_m (E_m - E_m^{R=1})^2}{\sum_m (E_m^{R=1})^2}} \tag{3.1}$$

Figure 3.1.1 shows the relative error for both boundary conditions at the outer edge, as a function of the radius R. For both boundary conditions type, the solution seems to be radius-independent for $R = 0.6m$.

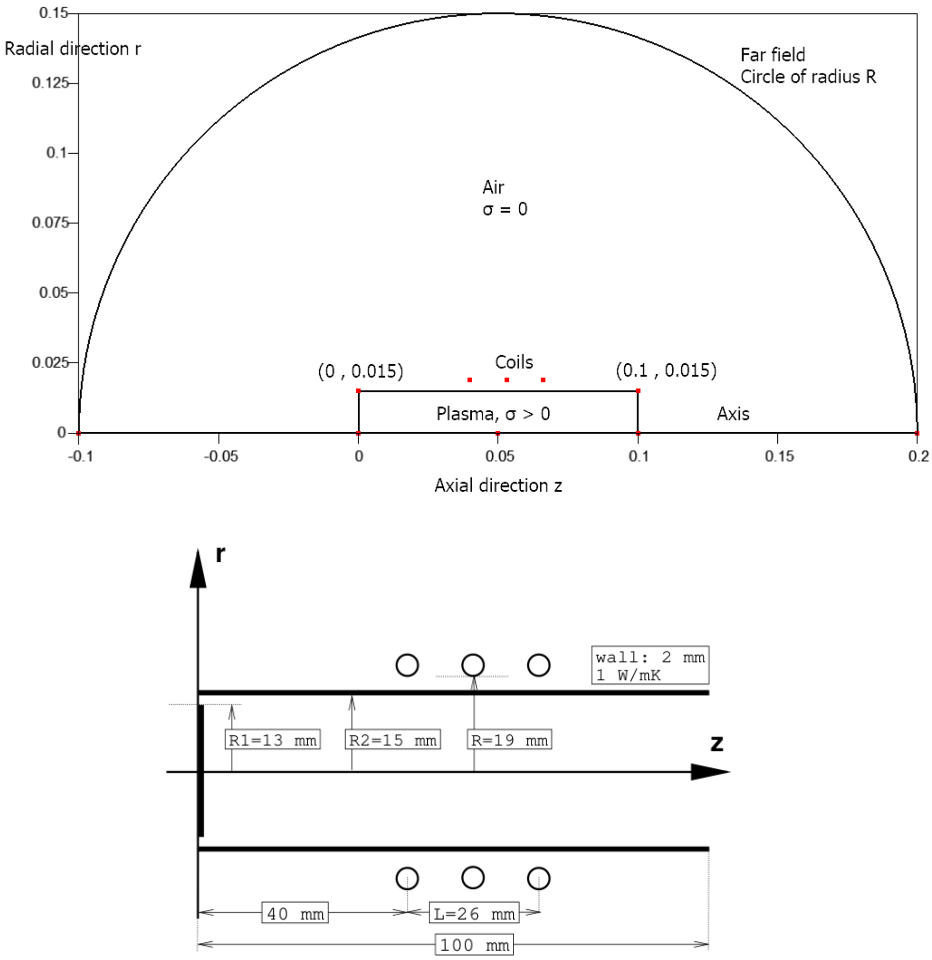

Figure 3.0.1: Geometry of the VKI minitorch (vanden Abeele [2]).

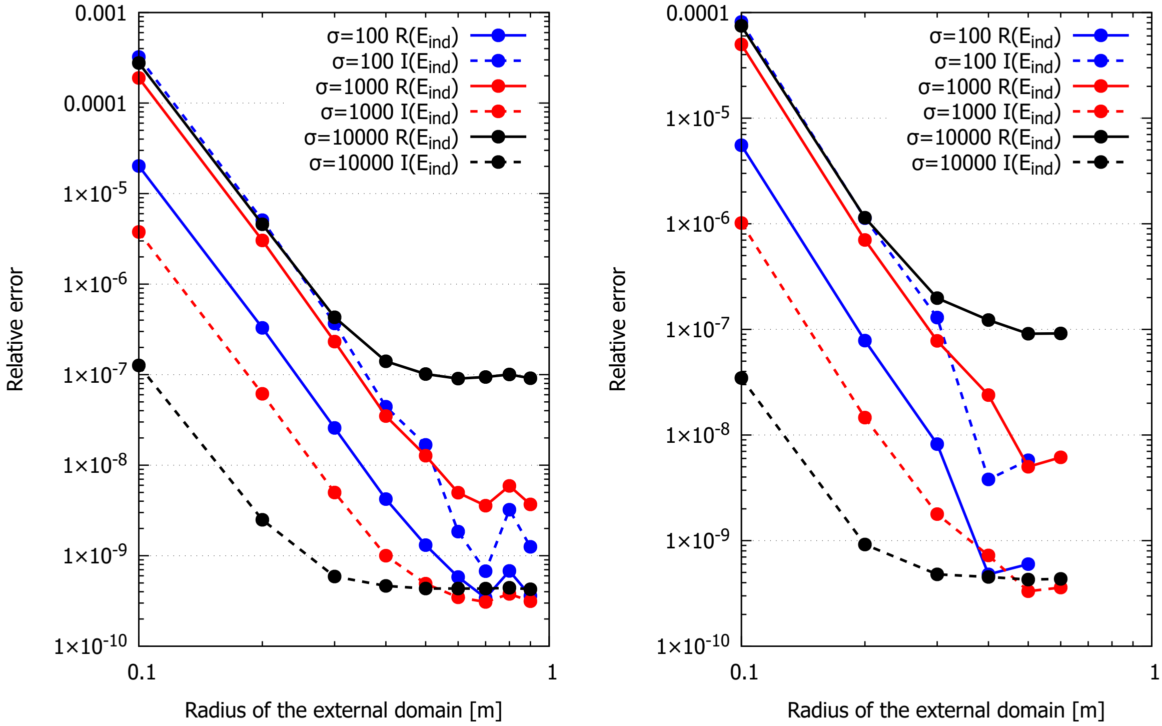

(a) $\frac{\partial E_{ind}}{\partial n} = 0$

(b) $E_{ind} = 0$

Figure 3.1.1: Influence of the size of the external domain on the solution. Cut at $z = 0.053m$ located at the middle coil.

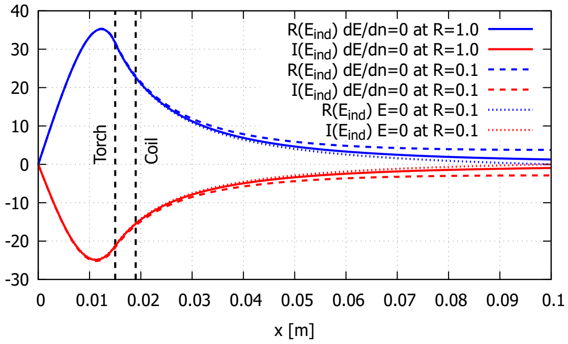

(a) $\sigma = 100S/m$

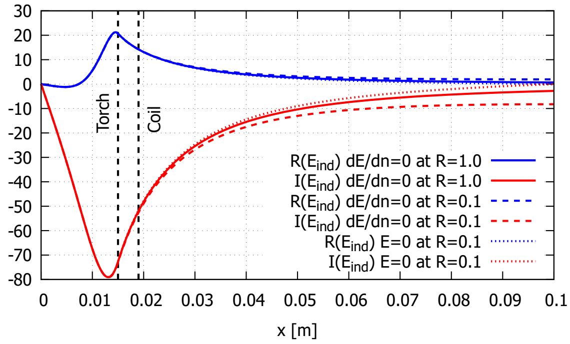

(b) $\sigma = 1000S/m$

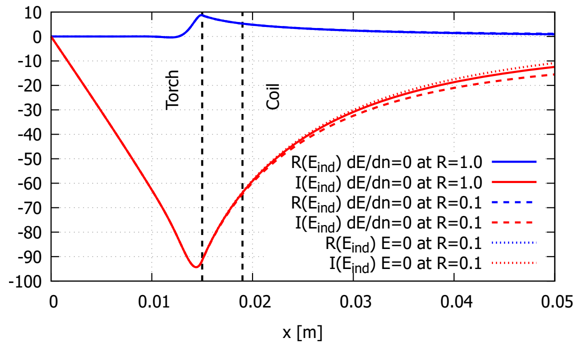

(c) $\sigma = 1000S/m0$

Figure 3.2.1: Influence of the boundary condition set on the external domain. Cut at $z = 0.053m$ located at the middle coil.

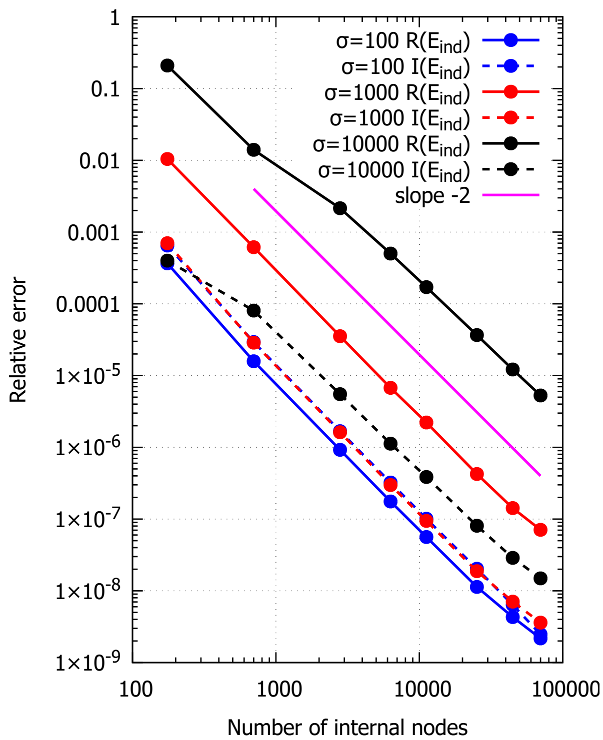

Figure 3.3.1: Convergence rate

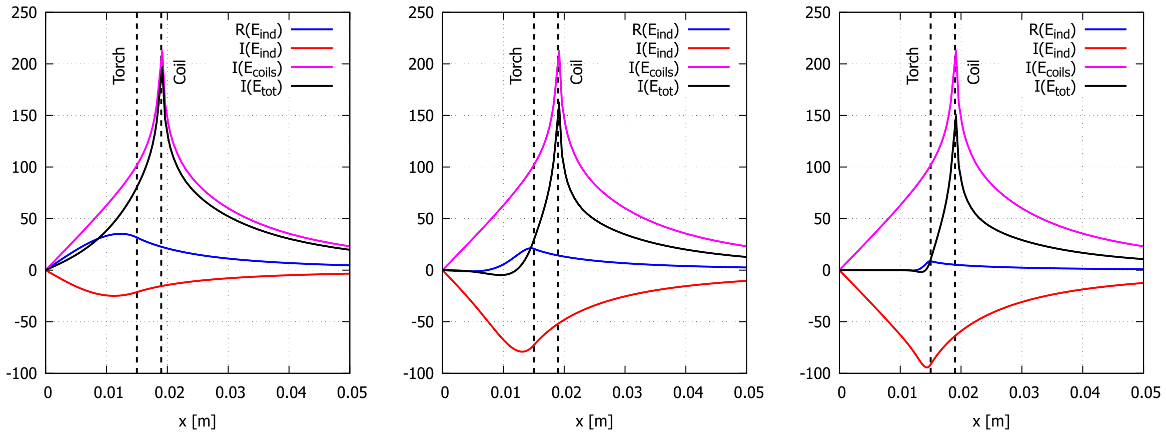

(a) $\sigma = 100S/m$ **(b)** $\sigma = 1000S/m$ **(c)** $\sigma = 10000S/m$

Figure 3.4.1: Influence of the electrical conductivity σ on the solution. Cut at $z = 0.053m$ located at the middle coil.

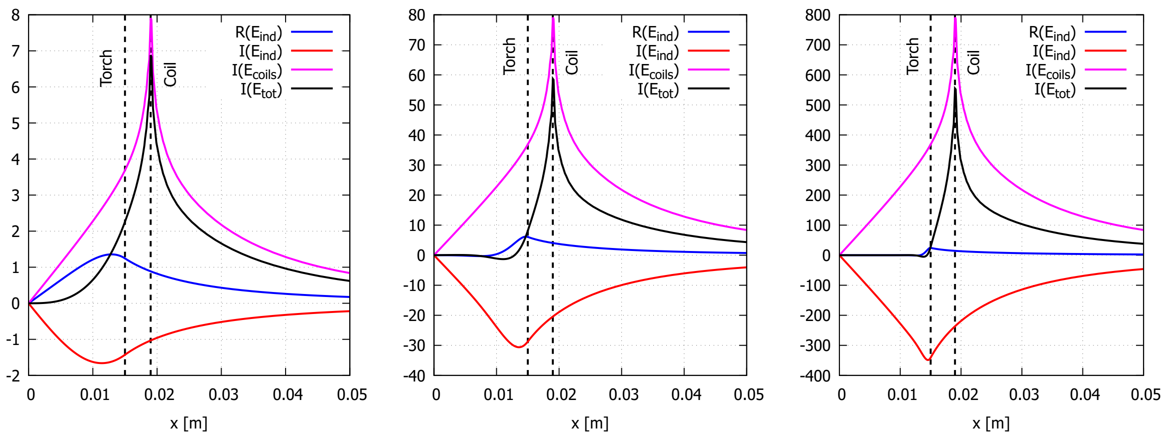

(a) $f = 10^6 Hz$ **(b)** $f = 10^7 Hz$ **(c)** $f = 10^8 Hz$

Figure 3.5.1: Influence of the excitation frequency f on the solution. Cut at $z = 0.053m$ located at the middle coil.

3.2 Influence of the boundary condition set on the external domain

3.3 Convergence rate

3.4 Influence of the electrical conductivity

3.5 Influence of the excitation frequency

Ecoil directly proportional to f

Bibliography

[1] J.W. McKelliget. A mathematical model of an inductive plasma torch. Technical Report 86-112.1, University of Lowell, College of Engineering, September 1986.

[2] David vanden Abeele. *An efficient computational model for inductively coupledair plasma flows under thermal and chemical non-equilibrium - with application to atmospheric re-entry flow studies*. PhD thesis, Katholieke Universiteit Leuven, 2000.

[3] Silvânia Lopes. *Integrated CFD Model for Nanoparticle Production in Inductively Coupled Plasma Reactors: Implementation and Application*. PhD thesis, Université Libres de Bruxelles, 2016.

[4] D. Bernardi, V. Colombo, G. G. M. Coppa, and A. D'Angola. Simulation of the ignition transient in rf inductively-coupled plasma torches. *The European Physical Journal D - Atomic, Molecular, Optical and Plasma Physics*, 14(3):337–348, 2001.

[5] Yves Detandt. *Extension of Spectral/Finite Element solver for Large Eddy Simulation (SFE-LES) for axisymmetric bodies*. PhD thesis, Université Libres de Bruxelles, 2004.